

Electronic Supplementary Information (ESI)

Electrochemically Switchable Polymerization from Surface-Anchored Molecular Catalysts

Miao Qi^{‡a}, Haochuan Zhang^{‡a}, Qi Dong^{‡a}, Jingyi Li^a, Rebecca A. Musgrave^b, Yanyan Zhao^a, Nicholas Dulock^a, Dunwei Wang^{*a}, and Jeffery A. Byers^{*a}

^a Department of Chemistry, Boston College, 2609 Beacon Street, Chestnut Hill, Massachusetts, 02467, United States

^b Department of Chemistry and Chemical Biology, Harvard University, Cambridge, Massachusetts 02138, United States

[‡] These authors contributed equally to this work.

Table of Contents

1. General Information and Procedures.....	3-4
2. Experimental Procedures	5-8
3. Size and dimensions of TiO ₂ -FTO electrode (Figure S1)	9
4. TGA of P25 TiO ₂ nanoparticles (Figure S2).....	9
5. Electron microscopy characterizations (Figure S3)	10
6. Polymerizations on P25 TiO ₂ nanoparticles (Figure S4-S7).....	10-12
7. Mössbauer spectroscopy (Figure S8).....	12
8. Cyclic voltammetry study of TiO ₂ -FTO electrode (Figure S9).....	13
9. Polymerizations on TiO ₂ -FTO electrode (Figure S10—S11).....	13-14
10. Contact angle measurements (Figure S12-S13)	14-15
11. Calculation of Mössbauer spectroscopy (Table S1-S3).....	16-21
12. References	22-23

1. General Information and Procedures

General Considerations. Unless stated otherwise, all reactions were carried out in oven-dried glassware in an Ar or N₂-filled glove box. Bis(imino)pyridine iron bisalkyl complex **1** was synthesized following literature procedures.¹ Solvents (dichloromethane, diethyl ether, pentane) were used after passage through alumina columns under a blanket of argon² or distilled over calcium hydride to remove water and then degassed briefly by exposure to vacuum. Methanol, hexanes, and acetone were purchased from Fisher Scientific and used without further purification. Titania P25 nanoparticles were purchased Sigma-Aldrich. (*rac*)-Lactide were obtained from Purac Biomaterials; and L-lactide was purchased from Natureworks. Racemic and enantiomerically enriched lactide were recrystallized from ethyl acetate followed by recrystallization from hot toluene and dried *in vacuo* over P₂O₅ prior to polymerization. Cyclohexene oxide was purchased from Acros Organics and distilled from calcium hydride prior to its use. Cyclic voltammetry and bulk electrolysis were carried out on a potentiostat (Biologic VMP3). Platinum wire, tetrabutylammonium hexafluorophosphate (>99%), lithium perchlorate (>99.99%), bis(trifluoromethane)sulfonimide lithium salt (LiTFSI, 99.95%), poly(vinylidene fluoride) (PVDF) Fluorine-doped tin oxide (FTO) coated glass and lithium metal ribbon (>99.9%) were purchased from Sigma-Aldrich. The glass cylinder with a fine frit used to house the counter electrode was prepared from literature reported procedures.³

Equipment and Analytical Methods. Nuclear magnetic resonance (NMR) spectra were recorded at ambient temperature (unless indicated otherwise) on spectrometers operating at 500 or 600 MHz for ¹H NMR. The line listing for NMR spectra of diamagnetic compounds are reported as follows: chemical shift (multiplicity, coupling constant, integration). Gel permeation chromatography (GPC) was performed on an Agilent GPC220 in THF at 40 °C with three PL gel columns (10 μm) in series. Molecular weights and molecular weight distributions were determined from the signal response of the RI detector relative to polystyrene standards. Refractive index increment (dn/dc) (0.042 mL/g for PLA and 0.085 mL/g for PCHO) used for GPC were obtained from literature.⁴ Centrifugation used for polymer purification was carried out using a Beckman Coulter J2-MC Centrifuge with Rotor 17.0 at 2500 RPM operating at 4°C for 20 minutes. UV-irradiation of the titanium nanoparticles were processed using the Model 42 UVO-Cleaner (Jelight Company Inc.). Atomic layer deposition (ALD) was conducted on Cambridge NanoTech (Savannah 100) system. High-angle annular dark field (HAADF)-scanning transmission electron microscopy (STEM) imaging and energy-dispersive X-ray spectroscopy (EDX) elemental mapping analyses were performed employing Tecnai G2 20 (200 keV, FEI). The HAADF-STEM images were acquired with a scan size of 1024 × 1024 pixels and a dwell time of 10 μs. The convergence semi-angle used was 21 mrad, and the camera length was 150 mm. Elemental analysis was performed using a windowless super-X SDD EDX detector operated using Aztec (Oxford Instrument) software. Fy-Light 130K airbrush kit (Amazon, Fy-Light) was used to prepare TiO₂-FTO plates. Inductively Coupled Plasma - Reactive Ion Etching (ICP-RIE, Plasma-ThermVersaline LL ICP) instrument was used to make the patterned electrode. Raman spectroscopy measurements were performed with Raman system (XploRA, Horiba) with a 532 nm laser excitation. ATR-FTIR spectra were recorded using a Bruker Vertex 70 FTIR spectrometer (Billerica, MA) equipped with an MCT detector (FTIR-16; Infrared Associates; Stuart, FL). The TiO₂ coated FTO glass slide was pressed on the Si or ZnSe ATR crystal. The absorbance was calculated with the air spectrum collected

before loading the sample as the reference. Zero-field ^{57}Fe Mössbauer spectra were measured with a constant acceleration spectrometer (SEE Co, Minneapolis, MN) at 90 K. Isomer shifts are quoted relative to Fe foil at room temperature. Data were analyzed and simulated with Igor Pro 6 software (WaveMetrics, Portland, OR) using Lorentzian fitting functions. Samples were prepared by suspending 20–50 mg of compound in sufficient Paratone oil immobilizing by rapid freezing in liquid nitrogen under nitrogen. All DFT calculations were performed with the ORCA program package.⁵ The geometry optimizations of the complexes and single-point calculations on the optimized geometries were carried out at the B3LYP level of DFT.^{6,7} Triple- ζ -quality basis sets TZVP were performed with all atoms.⁸⁻¹⁰ ^{57}Fe Mössbauer parameters (isomer shift δ and quadrupole splitting $|\Delta E_Q|$) were computed following the procedure reported by Neese *et al.*¹¹⁻¹³ Inductively coupled plasma optical emission (ICP-OES) spectrometry was recorded in an Agilent 5100 instrument that was calibrated using known concentrations of standard solutions to quantify Fe element. 1000 ppm Fe standard solution was purchased from Sigma-Aldrich. To digest iron-complex from Fe(II)-TiO₂, the powder/plate was soaked in 20 mL 1% nitric acid solution overnight. Then the solution was subjected to centrifugation and used for ICP-OES test. Thermal gravimetric analysis (TGA) was carried out on an STA 449 F1 Jupiter® from NETZSCH (NETZSCH-Gerätebau GmbH Wittelsbacherstraße 42 95100 Selb Germany); all measurements were performed under a constant flow of nitrogen (40 mL/min) and a heating rate of 20 °C/min. Contact angles of deionized water on polymer-modified TiO₂/FTO substrates were measured by a home-built instrument consisted of sample stage, lens, camera and a goniometer (Model 500, ramé-hart), and the data was fitted using ImageJ software.

2. Experimental Procedures

Calculating surface hydroxyl groups on the P25 TiO₂ powder. The density of surface hydroxyl groups was calculated based on reported literature.¹⁴ The temperature was first ramped up from 19 °C to 120 °C (T₁) and held at 120 °C for 20 min to remove the physisorbed water. The temperature was then increased from 120 °C to 500 °C (T₂) at a rate of 20 °C/min to measure the weight loss from removing the surface hydroxyl groups.

Anchoring complex 1 onto P25 TiO₂ powder (Fe(II)-TiO₂). Prior to bring the powder into a nitrogen filled glovebox, the TiO₂ powder was heated under reduced pressure (lower than 10⁻⁴ torr) at 150 °C to remove the surface bound water. The powder (100 mg) was then mixed with a solution of bis(imino)pyridine iron bisalkyl complex **1** (50 mg, 0.08 mmol) in diethyl ether (4 mL) for overnight in the glovebox in a 7-mL vial. The mixture was centrifuged to collect the powder. The powder was then washed with diethyl ether (2 mL × 3) and dichloromethane (2 mL) with centrifugation after each wash until the supernatant was colorless. The resulting powder was light purple in color. ICP-OES showed the iron concentration on the powder was 2.1 ± 0.3 wt%.

Surface-initiated polymerization of (rac)-lactide with the P25 Fe(II)-TiO₂. In a nitrogen-filled glove box, Fe(II)-TiO₂ (100 mg, 2.1 mg Fe, 0.038 mmol Fe) was suspended in a dichloromethane (2.00 mL) solution of (rac)-lactide (300 mg, 2.08 mmol) and 1,3,5-trimethoxy benzene (94.0 mg, 0.500 mmol) in a 20-mL vial. The mixture was allowed to stir vigorously at room temperature overnight. The mixture was centrifuged to separate the powder from the supernatant. The powder was washed with dichloromethane (5 mL) 3 times in the glovebox. Each wash was followed by centrifugation to ensure full recovery of the powder. 67% lactide conversion was observed with the ¹H NMR of the supernatant, by comparing the relative integration of the methine peaks of the remaining lactide (q, 5.0 ppm) to the methyl peaks of the internal standard (s, 3.8 ppm). Similar polymerization experiment was carried out with unfunctionalized P25 TiO₂ powders to rule out any detrimental background polymerization or interference by TiO₂. These reactions revealed no lactide polymerization with the TiO₂ powder that did not contain the Fe(II) complex.

Removing poly(lactic acid) from the surface of Fe(II)-TiO₂. On the bench in air, the solid product obtained from the surface-initiated polymerization of lactide was suspended in dichloromethane (2 mL) in 20-mL vial and precipitated in methanol (20 mL) to remove unreacted lactide monomer. The PLA-TiO₂ powder was collected by centrifugation, and suspended again in dichloromethane (5 mL) in a 20-mL vial. Iodomethane (0.2 mL, 0.46 g, 3.2 mmol) was dissolved in dichloromethane (10 mL). An aliquot of the iodomethane solution (1 mL, 0.046g, 0.32 mmol) was added to the suspension of the PLA-TiO₂ powder dropwise. The reaction mixture was allowed to stir at room temperature for 16 hours. The solvent was removed under vacuum. The remaining solid was then suspended in THF (10 mL) and washed 3 times with THF (20 mL), following each wash with centrifugation. The supernatant and washes were combined and the solvent was removed. The resulting solid was dried under vacuum and analyzed by ¹H NMR and GPC to get polymer composition and molecular weight, respectively.

Chemical oxidation of Fe(II)-TiO₂ to get Fe(III)-TiO₂. In a nitrogen-filled glove box, Fe(II)-TiO₂ (100 mg, 2.1 mg Fe, 0.038 mmol Fe) was suspended in dichloromethane (2 mL) in a 7-mL vial. In a second vial, FcPF₆ (125 mg, 0.38 mmol) was dissolved in dichloromethane (5 mL).

The FcPF₆ solution was then added to the suspension of the Fe(II)-TiO₂ powder, and the mixture was allowed to stir at room temperature for 30 min. The powder was isolated from the supernatant by centrifugation, and washed with dichloromethane (5 mL) for 3 times with centrifugation, until the supernatant was colorless. The powder was then dried under vacuum, and appeared to be light brown in color.

Surface-initiated polymerization of cyclohexene oxide with Fe(III)-TiO₂. In a nitrogen-filled glove box Fe(III)-TiO₂ powder (100 mg, 1.7 mg Fe, 0.030 mmol Fe) was suspended in a dichloromethane (2 mL) solution of cyclohexene oxide (500 mg, 5.10 mmol) and 1,3,5-trimethoxy benzene (94.0 mg, 0.500 mmol) in a 20-mL vial. The mixture was allowed to stir vigorously at room temperature overnight. The powder was separated from the supernatant by centrifugation and washed three times with dichloromethane (5 mL). Each wash was followed by centrifugation to ensure full recovery of the Fe(III)-TiO₂ powder. 33% epoxide conversion was observed with ¹H NMR, through the analysis of the supernatant by comparing the relative integration of the methine peaks of the remaining cyclohexene oxide (q, 3.0 ppm) to the methyl peaks of the internal standard (s, 3.8 ppm). The powder was then dried under vacuum at 10⁻³ torr overnight to remove unreacted cyclohexene oxide monomer. Similar polymerization experiment was carried out with unfunctionalized P25 TiO₂ powders to rule out any detrimental background polymerization or interference by TiO₂. These reactions revealed no cyclohexene oxide polymerization with the TiO₂ powder that did not contain the Fe(III) complex.

Removing poly(cyclohexene oxide) from the surface of Fe(III)-TiO₂. On the bench, the solid product obtained from the surface-initiated polymerization of cyclohexene oxide was suspended again in dichloromethane (5 mL) in a 20-mL vial. Iodomethane (0.20 mL, 0.46 g, 3.2 mmol) was dissolved in dichloromethane (10 mL). The iodomethane solution (1.0 mL, 0.046g, 0.32 mmol) was added to the suspension dropwise. The reaction mixture was allowed to stir at room temperature for 16 hours. The solvent was removed under vacuum, and the remaining solid was suspended in hexanes (10 mL) and washed three times with THF (20 mL) following each was with centrifugation. The resulting solid was dried under vacuum and analyzed by ¹H NMR and GPC to get polymer composition and molecular weight, respectively.

Preparation of TiO₂-FTO electrode. Preparation of TiO₂-FTO electrode was carried out following a previously reported method.¹⁵ First, 1.5 g commercial P25 TiO₂ nanopowder was mixed with 2.5 mL H₂O, 75 μL acetylacetone and 2 drops of Triton X-100 to make a uniform slurry. The slurry was then uniformly coated onto the FTO substrate (0.5 × 5 cm) by doctor blade method. Next, the plate was annealed at 450°C in air for 0.5 h. The plate was then treated under UV irradiation for 30 minutes. Such electrodes were used for the study of electrochemical property of surface-anchored iron-complex and the following polymerizations. To get more uniform and thinner TiO₂ layer for better characterization by Raman spectrometer, the compressed air spraying method was also utilized to spray TiO₂ layer onto the FTO substrate. Dimensions of the plate are shown in Figure S1.

Anchoring complex 1 on TiO₂-FTO electrode. In a nitrogen-filled glove box, TiO₂-FTO electrode was soaked into a solution of bis(imino)pyridine iron bisalkyl complex **1** (50 mg, 0.080 mmol) in diethyl ether (4 mL) in a 7-mL vial overnight. The plate was removed from the reaction mixture and washed three times with diethyl ether (4 mL). The plate was purple in color after

the treatment. ICP-OES showed the iron loading on the TiO₂-FTO electrode was 1.7 ± 0.5 wt% (0.031 ± 0.009 mg/cm²).

Preparation of the electrically discriminated two-strip TiO₂-FTO electrode. To prepare electrically discriminated electrode for patterned polymerization, ICP-RIE instrument was used to etched out the middle FTO layer into a 1mm width trench on FTO substrate (1 × 5 cm). As a result, two sides of the FTO electrode can be addressed separately by external electric potential. The TiO₂ layer was then coated on the etched FTO substrate by either doctor blade method or compressed air spraying method (Figure S1), following by anchoring iron complex **1** as described above.

Procedure for CV measurements. To prepare iron-functionalized electrodes for cyclic voltammetry study, ca. 10-50 nm TiO₂ layer was deposited on the titanium mesh according to previously reported method.¹⁶ CV of iron-complex anchored on ALD-TiO₂ was conducted using a three-electrode configuration, where the Fe(II)-TiO₂ was used as the working electrode, and two platinum wires served as the counter and reference electrodes. A 0.05 M solution of tetrabutylammonium hexafluorophosphate (TBAPF₆) in dichloromethane was used as the electrolyte. The scan rate was varied (20 mV/s to 500 mV/s) to study the diffusion process on the electrode. For control experiment, iron-functionalized TiO₂-FTO electrodes made from P25 nanopowder were also used as working electrode to conduct similar CV study (Figure S9).

Cell assembly for bulk electrolysis. Following a previously reported procedure,³ bulk electrolysis was carried out using a divided two-electrode configuration. All manipulations during the construction of the cell and the subsequent bulk electrolysis was carried out in an argon-filled glovebox. This cell used the iron(II) functionalized electrode as the working electrode and a lithium metal counter/reference electrode isolated from the working electrode by a Li⁺/PVDF membrane coated fritted tube. A 0.05 M solution of LiClO₄ in dimethoxy ether (1 mL) was added to the tube as the electrolyte. The top of the lithium rod was affixed to the tube with Teflon tape. For the working electrode chamber, a 0.05 M solution of TBAPF₆ in dichloromethane was used as the electrolyte. The electrical connection to the potentiostation was established by alligator clips affixed to the top of the Fe(II)-TiO₂ plate as the working electrode and the Li counter/reference electrode. An oxidizing potential of 1.0 V vs Fc/Fc⁺ was applied to the working electrode for at least one hour, until the current dropped below 3 μA.

Oxidation of the iron(II) modified TiO₂-FTO electrode with FcPF₆. In a nitrogen-filled glove box, the iron(II) modified TiO₂-FTO electrode plate was exposed to a solution of FcPF₆ (25 mg, 0.076 mmol) dissolved in dichloromethane (2 mL). The plate was removed from the solution and rinsed four times with diethyl ether (3 mL). The color of the plate was brown after the oxidation.

Surface-initiated polymerization of lactide on the iron(II) modified TiO₂-FTO electrode. In an argon-filled glovebox, the iron(II) modified TiO₂-FTO electrode plate was placed in a dichloromethane (10 mL) solution containing lactide (500 mg, 3.47 mmol) and 1,3,5-trimethoxy benzene (336 mg, 2.00 mmol) in a 20-mL vial. The mixture was stirred at 350 rpm at room temperature overnight. Lactide conversion (20%) was determined from the ¹H NMR by comparing the relative integration of the methine peaks of the remaining lactide (q, 5.0 ppm) to the methyl peaks of the internal standard (s, 3.8 ppm) in the supernatant.

Surface-initiated polymerization of cyclohexene oxide on the iron(III) modified TiO₂-FTO electrode. In an argon-filled glovebox, the iron(II) modified TiO₂-FTO electrode plate was

first electrochemically oxidized into iron(III) following above electrolysis procedure. Then the iron(III) modified TiO₂-FTO electrode plate was placed in a dichloromethane (10 mL) solution containing cyclohexene oxide (1.37 g, 14.0 mmol) and 1,3,5-trimethoxy benzene (336 mg, 2.00 mmol) in a 20-mL vial. The mixture was stirred at 350 rpm at room temperature overnight. Cyclohexene oxide conversion (15%) was determined from the ¹H NMR by comparing the relative integration of the methine peaks of the remaining cyclohexene oxide (q, 3.0 ppm) to the methyl peaks of the internal standard (s, 3.8 ppm) in the supernatant.

Simultaneous surface-initiated polymerization of lactide and cyclohexene oxide on the electrically discriminated two-strip plate. In an argon-filled glovebox, one side of the electrically discriminated electrode plate was first electrochemically oxidized into iron(III) following above electrolysis procedure. The plate was washed three times with diethyl ether (4 mL), and then placed in a dichloromethane (10 mL) solution containing lactide (500 mg, 3.47 mmol), cyclohexene oxide (1.37 g, 14.0 mmol), and 1,3,5-trimethoxy benzene (336 mg, 2.00 mmol) in a 20-mL vial. The reaction was allowed to stir at 350 rpm at room temperature overnight. Lactide conversion (21%) was determined from the ¹H NMR of the supernatant by comparing the relative integration of the methine peaks of the remaining lactide (q, 5.0 ppm) to the methyl peaks of the internal standard (s, 3.8 ppm). Cyclohexene oxide conversion (13%) was determined from the ¹H NMR by comparing the relative integration of the methine peaks of the remaining cyclohexene oxide (q, 3.0 ppm) to the methyl peaks of the internal standard (s, 3.8 ppm) in the supernatant.

Sequential surface-initiated polymerization of lactide and cyclohexene oxide on the electrically discriminated plate. In an argon-filled glovebox, one side of the electrically discriminated electrode plate was first electrochemically oxidized into iron(III) following above electrolysis procedure. The plate was first placed in a dichloromethane (10 mL) solution containing lactide (500 mg, 3.47 mmol) and 1,3,5-trimethoxy benzene (336 mg, 2.00 mmol) in a 20-mL vial. The reaction was allowed to stir at 350 rpm at room temperature for 12 h. Lactide conversion (31%) was determined from the ¹H NMR of the supernatant from the first step by comparing the relative integration of the methine peaks of the remaining lactide (q, 5.0 ppm) to the methyl peaks of the internal standard (s, 3.8 ppm) in the supernatant. The plate was rinsed with dichloromethane (5 mL) and then placed in a dichloromethane (10 mL) solution of cyclohexene oxide (1.37 g, 14.0 mmol) and 1,3,5-trimethoxy benzene (336 mg, 2.00 mmol). The reaction was allowed to stir at 350 rpm at room temperature for 12 h. Cyclohexene oxide conversion (19%) was determined from the ¹H NMR of the supernatant from the second step by comparing the relative integration of the methine peaks of the remaining cyclohexene oxide (q, 3.0 ppm) to the methyl peaks of the internal standard (s, 3.8 ppm) in the supernatant.

3. Figures and Tables

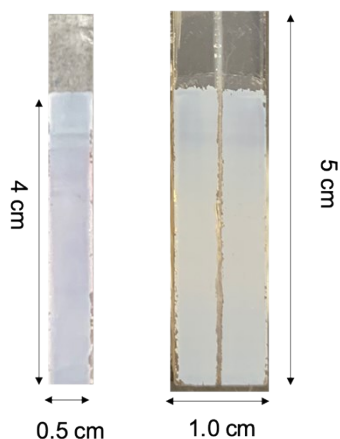


Figure S1. Size and dimensions of the TiO₂-FTO electrode (a) and TiO₂-FTO electrically discriminated plate (b).

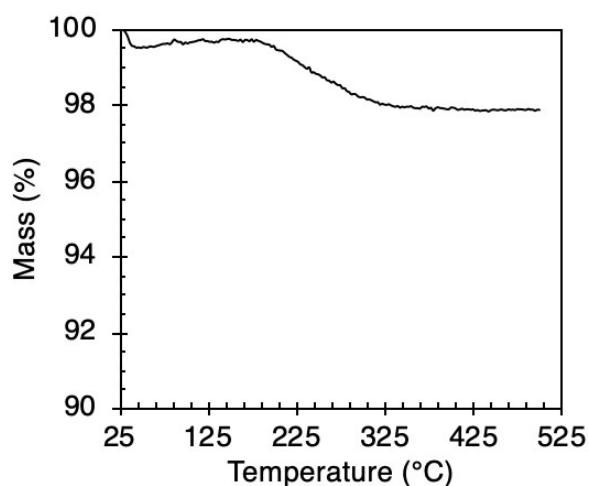


Figure S2. TGA of P25 TiO₂ nanoparticles after UV/water treatment.

The density of surface hydroxyl groups was calculated based on reported literature.¹⁴ The temperature was first ramped up from 19 °C to 120 °C (T_1) and held at 120 °C for 20 min to remove the physisorbed water. The temperature was then increased from 120 °C to 500 °C (T_2) at a rate of 20 °C/min to measure the weight loss from removing the surface hydroxyl groups. The calculation of the surface hydroxyl groups is done based on the hypothesis that the surface is free of hydroxyl groups at 500 °C

$$\# \text{ of } \frac{OH}{nm^2} = 2 \times 0.625 \times (wt_{T_1} - wt_{T_2}) \times N_A / (SSA \times wt_{T_1} \times MW_{H_2O})$$

The specific surface area of 50 m²/g was used to calculate the value. 0.625 is the calibration factor. wt_{T_1} and wt_{T_2} are the weight loss at 120 °C and 500 ° to calibrate the weight loss of chemisorbed water below 120 °C. MW_{H_2O} is the molecular weight of water, N_A is the Avogadro constant.

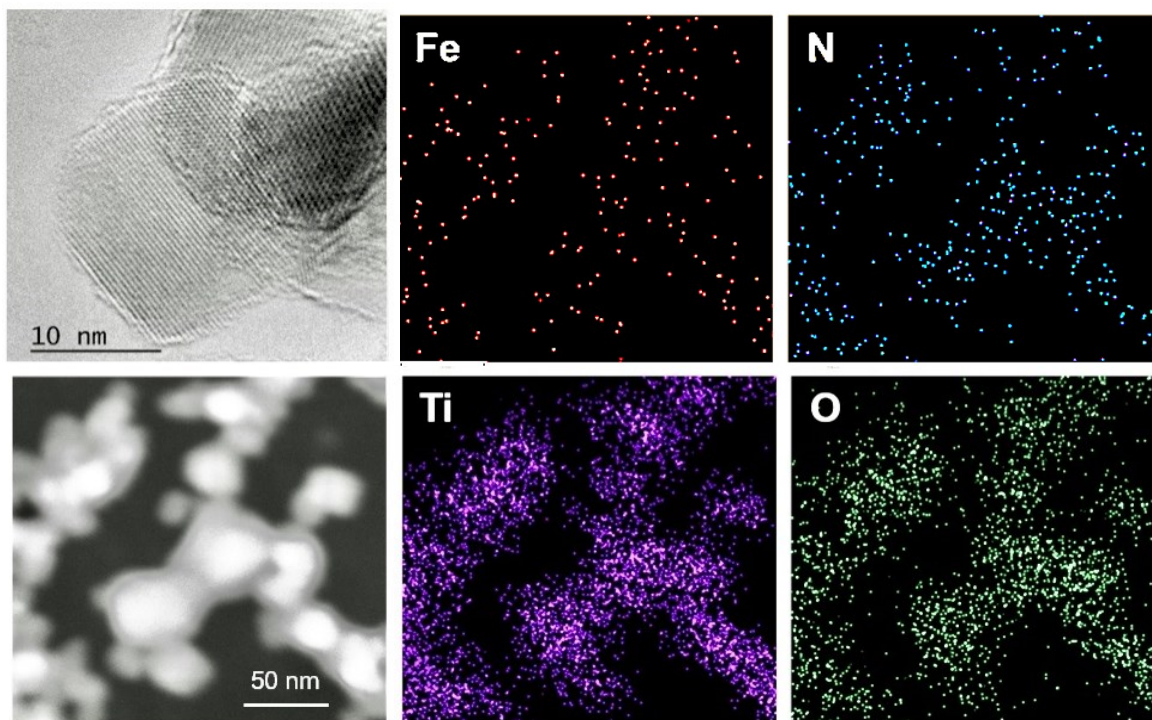


Figure S3. Electron microscopy characterizations. TEM image (a) and STEM elemental mapping images (b-f) of Fe-complex supported P25 TiO₂ nanoparticles

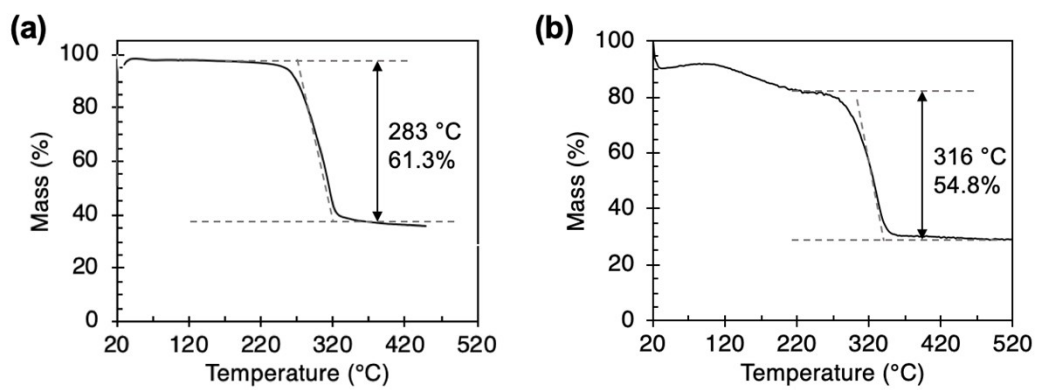


Figure S4. TGA of polymer-modified TiO₂ powder: a) PLA-modified TiO₂ powder; a) PCHO-modified TiO₂ powder.

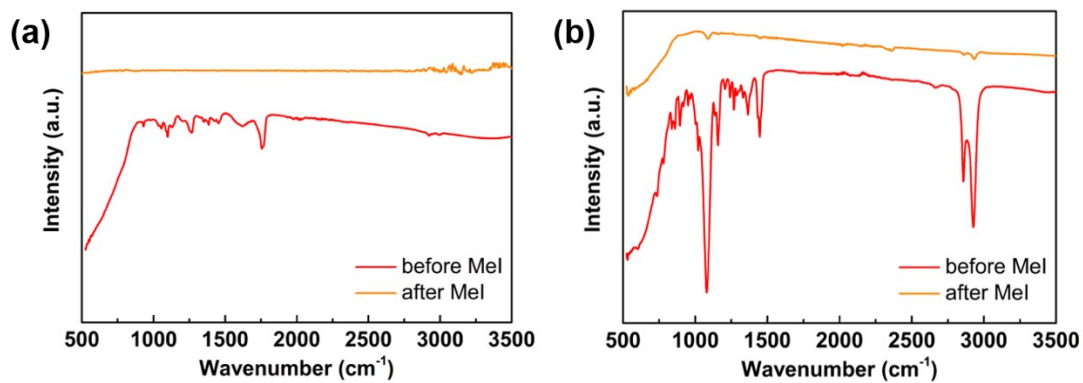


Figure S5. IR spectra of a) Fe(II)-TiO₂ powder with lactide polymerization; b) Fe(III)-TiO₂ powder with poly(cyclohexene oxide) polymerization.

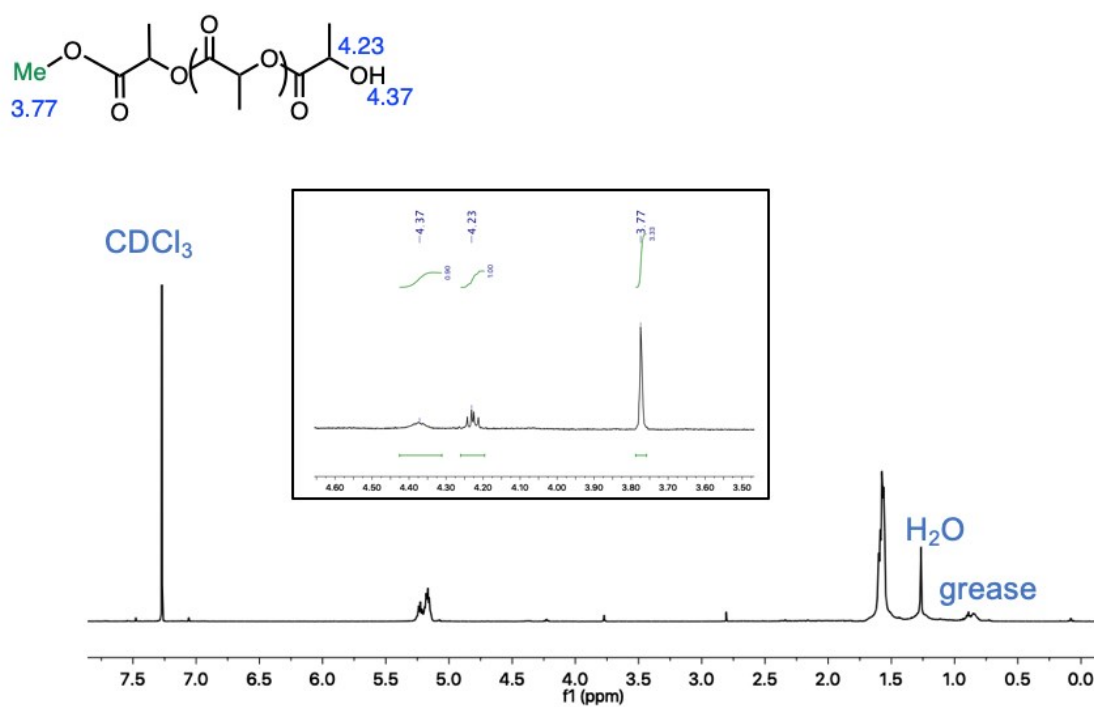


Figure S6. ¹H-NMR of the PLA after reacting with iodomethane to cleave the chain off the TiO₂ surface.

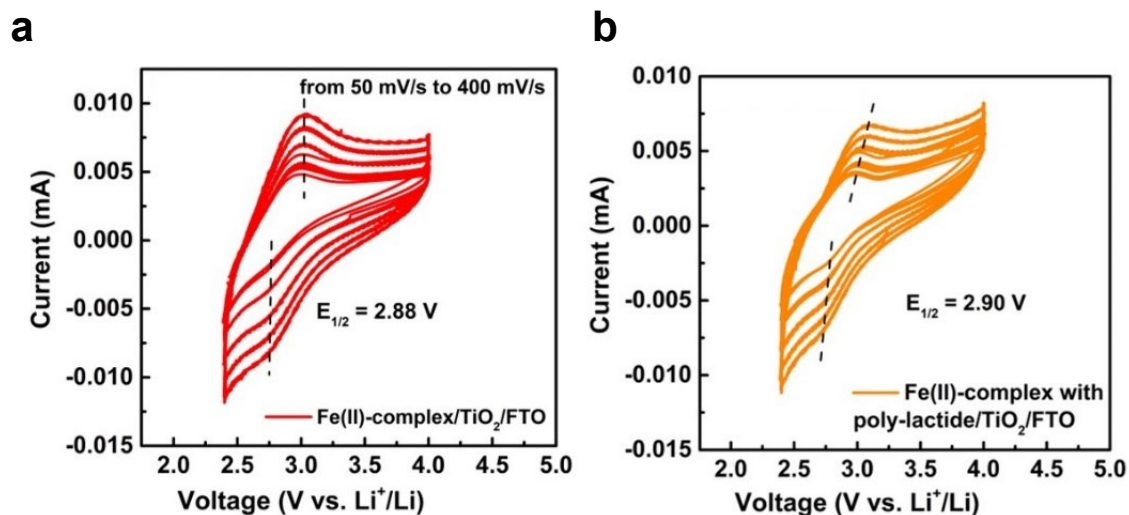


Figure S9. Cyclic voltammetry of Fe(II)-TiO₂ plate prepared with P25 nanoparticle; a) before lactide polymerization; b) after lactide polymerization

We hypothesized that the redox-active iron center would propagate away from the electrode surface during the polymerization process. Diffusion would affect the electron transfer process on the working electrode after the polymerization as the iron center will no-longer be attached to the electrode surface. Cyclic voltammetry show that with increased scan rates (from 20 mV/s to 500 mV/s, peak separation increased with the Fe(II)-PLA-TiO₂ plate, indicating the electron transfer process redox active center was diffusion limited. However, such effect is more pronounced at the anodic reaction and less obvious for the cathodic wave. This observation might reveal some interesting configuration of the polymer.

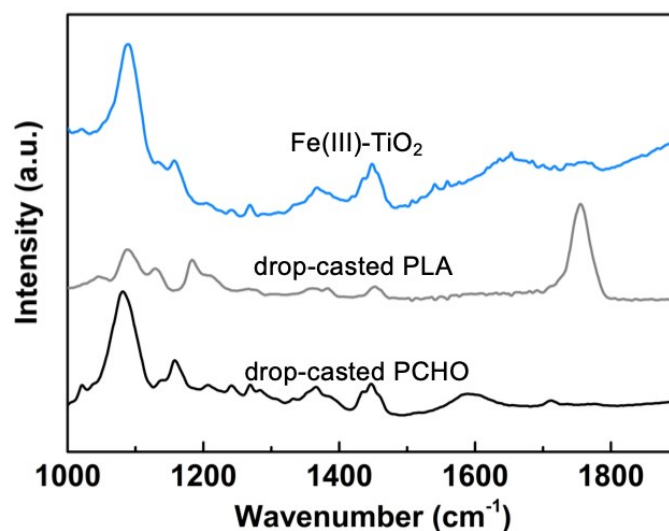


Figure S10. IR spectra of chemically oxidized Fe(III) modified TiO₂ glass substrate soaked in a mixture solution of lactide and cyclohexene oxide monomers.

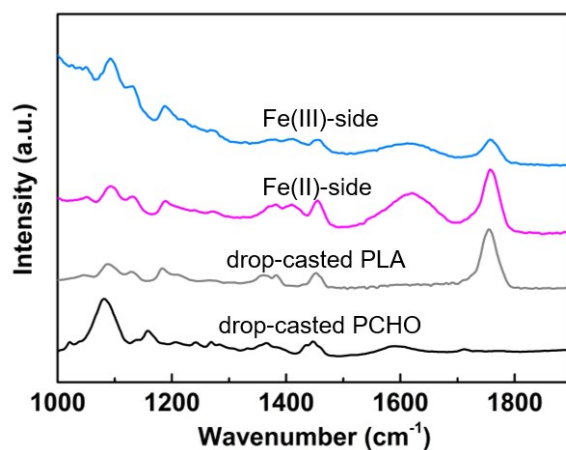


Figure S11. IR analysis of the binarily functionalized electrically discriminated plate obtained by soaking the plate into a mixture solution of lactide and cyclohexene oxide. On the Fe(III)-side of the plate, signals from PCHO predominate although PLA can also be observed. In contrast, on the Fe(II)-side of the plate, signals from PLA predominate.

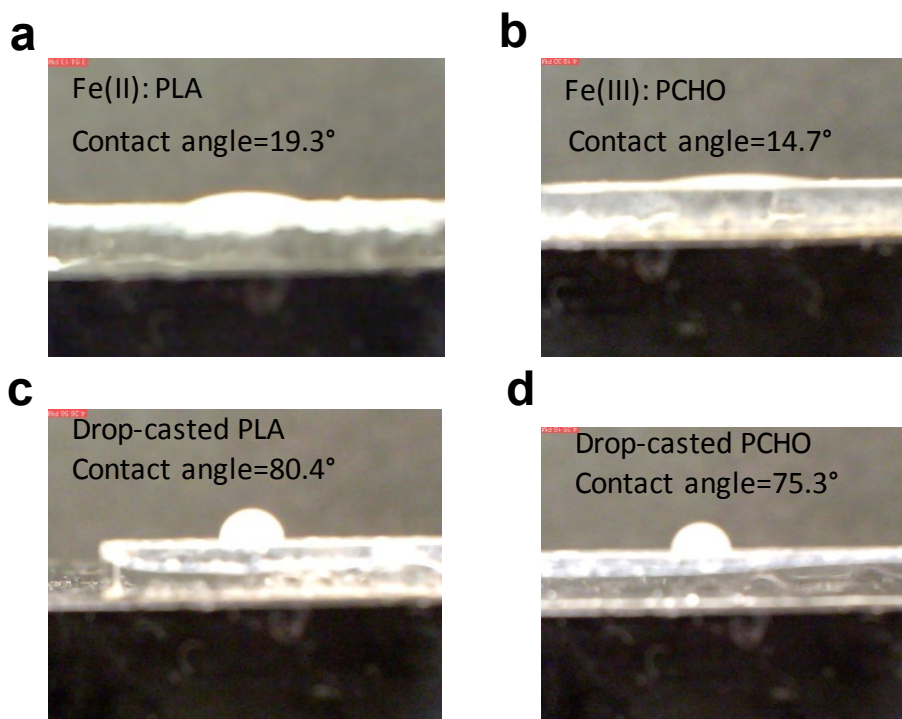


Figure S12. Surface water contact angle measurements of polymer-modified electrically discriminated electrode. a) Fe(II)-side, PLA-modified TiO_2 surface on the A side of the plate; b) Fe(III)-side, PCHO-modified TiO_2 surface on the B side of the plate; c) drop-casted PLA and d) drop-casted PCHO on FTO plate.

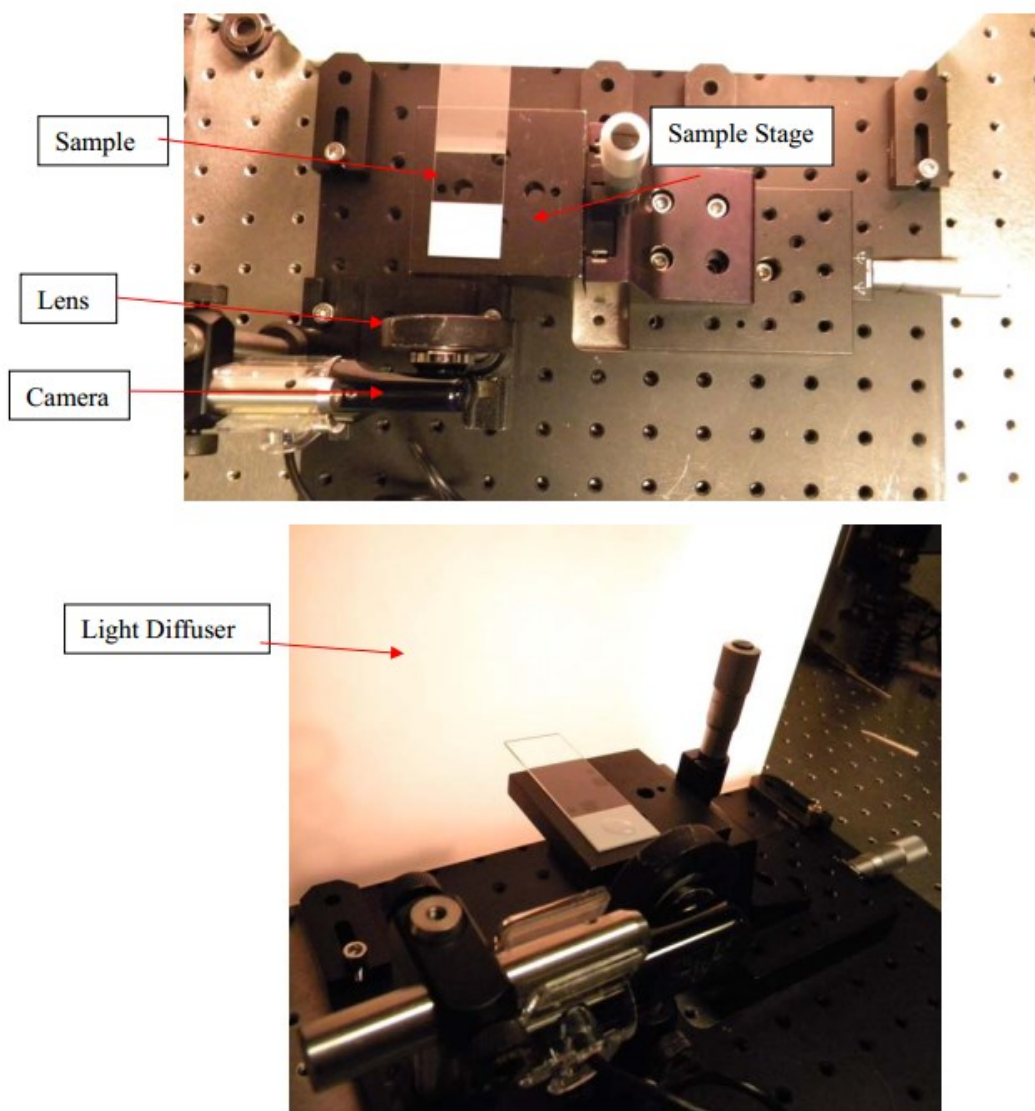


Figure S13. Home-made microscope stage used for contact angle measurements.

Table S1. Mössbauer parameters from ORCA calculations

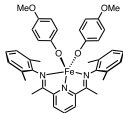
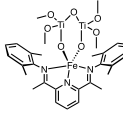
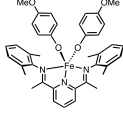
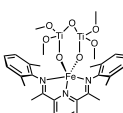
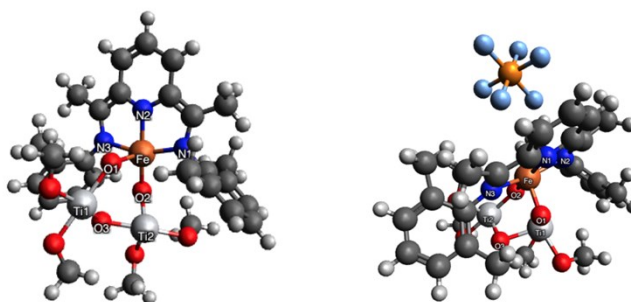
complex	complex	δ (mm/s)	$ \Delta E_Q $ (mm/s)
		calculated	calculated
2		0.926	1.938
S2		1.041	2.110
3		0.453	0.698
S3		0.455	0.980

Table S2. Calculated structures and selected bond angles and bond distances of a) Fe(II)-bis-titanoxide complex **S2** and complex **S3**.



S2

S3

Complex	O1-Fe-O2 (°)	Ti-O3-Ti (°)	N1-Fe-N2 (°)	N2-Fe-N3 (°)	N1-Fe-N3 (°)	Fe-N1(Å)	Fe-N2(Å)	Fe-N3(Å)
S2	100.8	118.1	81.2	77.3	158.2			
S3	95.8	93.7	79.2	154.5	75.4			
	Fe-O(1) (Å)	Fe-O(2) (Å)	Ti(1)-O(3) (Å)	Ti(2)-O(3) (Å)	Ti(1)-Ti(2) (Å)			
S2	1.956	2.041	1.938	1.928	3.316	2.509	1.945	2.018
S3	1.898	1.993	2.012	1.974	2.907	2.018	2.029	2.164

Table S3. Cartesian coordinates for the model Fe(II)-titanium ester complex **S2** obtained from DFT calculations.

Element			
Fe	6.37015	13.06013	6.96409
O	5.67708	11.72103	8.33975
N	7.30990	14.49279	8.10599
N	4.93820	14.32392	7.32993
N	4.90675	12.19330	5.87735
C	6.99769	16.88521	9.07774
H	8.06647	16.82124	9.35914
H	6.40882	17.07774	9.99823
H	6.88717	17.75103	8.38898
C	6.49007	15.63083	8.39588
C	5.23877	15.52985	7.97274
C	4.18597	16.60420	8.07317
C	2.90247	16.33154	7.32903
H	2.13632	17.10150	7.32232
C	2.69435	15.18374	6.65609
H	1.75920	15.06516	6.11865
C	3.74956	14.12761	6.61257
C	3.71185	13.01288	5.85975
C	2.52143	12.74592	4.95849
H	2.64059	11.82658	4.35444
H	2.39468	13.59004	4.24626
H	1.59307	12.66696	5.56414
C	8.64702	14.46258	8.56201
C	9.69537	14.94694	7.75240
C	11.01634	14.86555	8.22701
H	11.84366	15.20834	7.61901
C	11.27936	14.37555	9.50921
H	12.29684	14.33086	9.87445
C	10.22961	13.99338	10.34432
H	10.44659	13.67033	11.35508
C	8.90836	14.04189	9.88376
C	9.40960	15.62217	6.42861
H	10.34665	15.83628	5.86979
H	8.90406	16.58919	6.62531
H	8.71433	15.05216	5.78462
C	7.77296	13.70006	10.81608
H	7.11680	14.59169	10.93355
H	8.13450	13.43418	11.83128
H	7.16919	12.86413	10.41280
C	5.00070	10.94811	5.21339

C	4.16295	9.87193	5.60521
C	4.33266	8.61970	5.00646
H	3.71846	7.78184	5.31214
C	5.29354	8.44172	4.01124
H	5.41304	7.47165	3.55180
C	6.09965	9.51031	3.61169
H	6.84076	9.37182	2.83793
C	5.96093	10.75737	4.21852
C	3.13743	10.02580	6.69607
H	3.62784	10.51485	7.54381
H	2.71298	9.05693	7.02898
H	2.28469	10.65078	6.38591
O	7.72938	11.98452	6.05846
H	6.59325	11.57883	3.90759
Ti	6.13686	9.66645	8.54601
Ti	8.8978	10.93888	7.22199
O	7.40448	9.72770	7.08155
O	4.68551	9.20082	9.83873
C	3.81395	10.15886	10.32670
O	6.56390	7.70796	8.71502
C	7.87855	7.34306	8.39371
O	10.50059	12.11218	7.07082
C	10.51021	12.62322	5.75595
O	9.73516	9.79374	5.81834
C	10.58223	8.86011	6.44894
H	3.12347	9.60561	11.00337
H	3.15782	10.59206	9.55844
H	4.37403	10.89000	10.92719
H	8.02395	6.27851	8.68290
H	8.62517	7.94412	8.94921
H	8.02134	7.37896	7.29708
H	11.62897	8.97486	6.08765
H	10.24270	7.82934	6.21248
H	10.58109	8.99038	7.55111
H	11.36996	13.30431	5.59195
H	9.60560	13.19935	5.58073
H	10.53008	11.83303	4.98587
H	4.33371	17.46964	8.61558

Energy = -4739.597229017931 A.U.

Table S4. Cartesian coordinates for the model Fe(III)-titanium ester complex **S3** obtained from DFT calculations.

Element			
Fe	18.76896	5.77025	4.00585
O	18.44412	7.41859	3.12339
O	17.33529	5.98834	5.37325
N	20.39824	5.55728	2.83356
N	20.33666	6.16837	5.23134
N	17.85009	5.16195	2.14349
C	21.62659	5.66928	3.39469
C	22.78805	5.37423	2.65287
H	23.77945	5.49042	3.05985
C	22.65611	4.83656	1.38033
C	20.24346	5.0613	1.59085
C	18.86894	4.82729	1.17539
C	16.49653	5.15702	1.6241
C	15.83285	3.90733	1.40181
C	14.55075	3.86483	0.83918
H	14.04735	2.91654	0.70027
C	13.91785	5.02014	0.41521
H	12.9307	4.96505	-0.02777
C	14.59027	6.22963	0.47155
C	15.88211	6.32011	1.02963
C	16.48733	2.57083	1.64916
H	15.84331	1.90555	2.24953
H	17.48998	2.65352	2.1135
H	16.61787	2.06848	0.66545
C	16.58513	7.64292	0.83257
H	16.78873	8.17164	1.76769
C	21.62923	6.00511	4.67028
C	22.88624	6.04605	5.51688
H	22.65543	6.27969	6.57325
H	23.35047	5.03581	5.51634
C	20.13592	6.83415	6.47764
C	20.52435	8.20892	6.58754
C	20.25698	8.91474	7.76963
H	20.53471	9.95917	7.86877
C	19.61303	8.29299	8.83084
H	19.40642	8.85494	9.73425
C	19.24409	6.95189	8.73621
H	18.76159	6.49248	9.58762
C	19.50761	6.20813	7.57087
C	21.18161	8.96874	5.45135
H	22.17509	8.55703	5.20718

H	21.35197	10.03865	5.70383
H	20.54197	8.93236	4.54612
C	19.17259	4.74707	7.538
H	18.54354	4.47641	6.67534
H	18.65452	4.42897	8.46573
H	20.12292	4.18252	7.46908
P	20.99881	1.73899	4.48982
F	21.10043	0.26118	3.62214
F	19.4175	1.32493	5.0178
F	20.89945	3.2125	5.35384
F	22.57891	2.16035	3.96297
F	21.66416	0.97483	5.87676
F	20.3312	2.50092	3.10639
C	18.6016	4.13649	-0.15378
H	14.10242	7.09567	0.03533
H	15.97945	8.34905	0.21794
H	17.51791	7.4688	0.25024
H	23.62198	6.78196	5.13876
Ti	17.3836	8.06983	4.74109
Ti	15.35984	6.10418	5.44258
O	15.6946	7.33273	3.9344
O	17.38567	9.90907	4.0873
C	18.05009	10.54364	5.15334
O	13.3789	6.21716	5.49135
O	15.06225	4.57929	4.25915
C	16.11937	3.71459	4.55025
O	16.37653	8.51304	6.45134
C	15.07021	9.00899	6.23983
H	15.88574	2.69384	4.22936
H	16.37565	3.68441	5.62647
H	16.99309	4.07718	4.00798
C	13.00117	5.68391	6.7391
H	12.12046	5.01679	6.61761
H	12.74458	6.49849	7.4529
H	13.82806	5.07911	7.17128
H	14.80209	9.72839	7.04717
H	14.31797	8.20626	6.31418
H	14.97995	9.53492	5.27217
H	17.39898	11.2051	5.75983
H	18.94267	11.07197	4.7636
H	18.44762	9.76761	5.83855
C	21.38207	4.66021	0.85083
H	23.53484	4.51352	0.82398
H	21.31457	4.17693	-0.10408

H	19.52419	4.00589	-0.67978
H	17.9383	4.73687	-0.74071
H	18.15432	3.18095	0.02449

Energy = -5720.921268875836 A.U.

4. Reference

1. Biernesser, A. B.; Li, B.; Byers, J. A. Redox-controlled polymerization of lactide catalyzed by bis(imino)pyridine iron bis(alkoxide) complexes. *J. Am. Chem. Soc.* **2013**, *135*, 16553–16560.
2. Pangborn, A. B.; Giardello, M. A.; Grubbs, R. H.; Rosen, R. K.; Timmers, F. J. Safe and convenient procedure for solvent purification. *Organometallics* **1996**, *15*, 1518–1520.
3. Qi, M.; Dong, Q.; Wang, D.; Byers, J. A. Electrochemically Switchable Ring-Opening Polymerization of Lactide and Cyclohexene Oxide. *J. Am. Chem. Soc.* **2018**, *140*, 5686–5690.
4. Dorgan, J. R.; Janzen, J.; Knauss, D. M.; Hait, S. B.; Limoges, B. R.; Hutchinson, M. H. Fundamental solution and single-chain properties of polylactides. *J. Polym. Sci., Part B: Polym. Phys.* **2005**, *43*, 3100–3111.
5. Neese F. Wiley Interdiscip. Rev.: Comput. Mol. Sci. **2012**, *2*, 73–78.
6. Becke, A. D. Becke's three parameter hybrid method using the LYP correlation functional. *J. Chem. Phys.* **1993**, *98*, 5648–5652.
7. Lee, C.; Yang, W.; Parr, R. G. Development of the Colle-Salvetti correlation-energy formula into a functional of the electron density. *Phys. Rev. B* **1988**, *37*, 785–789.
8. Schäfer, A.; Huber, C.; Ahlrichs, R. Fully optimized contracted Gaussian basis sets for atoms Li to Kr. *J. Chem. Phys.* **1994**, *100*, 5829–5835.
9. Feller, D. The role of databases in support of computational chemistry calculations. *J. Comput. Chem.* **1996**, *17*, 1571–1586.
10. Weigend, F.; Ahlrichs, R. Balanced basis sets of split valence, triple zeta valence and quadruple zeta valence quality for H to Rn: Design and assessment of accuracy. *Phys. Chem. Chem. Phys.* **2005**, *7*, 3297–3305.
11. Römelt, R.; Ye, S.; Neese, F. Calibration of Modern Density Functional Theory Methods for the Prediction of ⁵⁷Fe Mössbauer Isomer Shifts: Meta-GGA and Double-Hybrid Functional. *Inorg. Chem.* **2009**, *48*, 784–785.
12. McWilliams, S. F.; Brennan-Wydra, E.; MacLeod, C.; Holland, P. L. Density Functional Calculations for Prediction of ⁵⁷Fe Mössbauer Isomer Shifts and Quadrupole Splittings in β-Diketiminato Complexes. *ACS Omega* **2017**, *2*, 2594–2606.
13. Delle Chiaie, K. R.; Biernesser, A. B.; Ortuno, M. A.; Dereli, B.; Iovan, D. A.; Wilding, M. J. T.; Li, B.; Cramer, C. J.; Byers, J. A. The role of ligand redox non-innocence in ring-opening polymerization reactions catalysed by bis(imino)pyridine iron alkoxide complexes. *Dalton Trans.* **2017**, *46*, 12971–12980.
14. Mueller, R.; Kammler, H. K.; Wegner, K.; Pratsinis, S. E. OH Surface Density of SiO₂ and TiO₂ by Thermogravimetric Analysis. *Langmuir* **2002**, *19*, 160–165.
15. Nazeeruddin, M. K.; Kay, A.; Rodicio, I.; Humphry-Baker, R.; Mueller, E.; Liska, P.; Vlachopoulos, N.; Graetzel, M. Conversion of light to electricity by cis-X₂bis(2, 2'-bipyridyl-4, 4'-dicarboxylate) ruthenium (II) charge-transfer sensitizers (X= Cl-, Br-, I-, CN-, and SCN-) on nanocrystalline titanium dioxide electrodes. *J. Am. Chem. Soc.* **1993**, *115*, 6382–6390.

16. Lin, Y. J.; Zhou, S.; Liu, X. H.; Sheehan, S. W.; Wang, D. W. TiO₂/TiSi₂ Heterostructures for High-Efficiency Photoelectrochemical H₂O Splitting. *J. Am. Chem. Soc.* **2009**, 131 (8), 2772–2773.